SHAPE OPTIMIZATION OF SHELLS CONSIDERING STRAIN ENERGY AND ALGEBRAIC INVARIANTS OF PARAMETRIC SURFACE

Shinnosuke Fujita[1] **and Makoto Ohsaki**[2]
1) Graduate Student, Kyoto University, Kyoto, Japan
2) Associate Professor, Kyoto University, Kyoto, Japan

ABSTRACT

A new approach is proposed for shape optimization of shell structures, where requirements on the aesthetic aspect and the constructability as well as the structural rationality are simultaneously considered in the problem formulation. The surface shape is modeled using a tensor-product Bézier surface to reduce the number of variables, while the ability to generate moderately complex shape is maintained. The strain energy is used to represent the mechanical performance, and the aesthetic properties and smoothness of the surface are quantified by algebraic invariants of the surface. The condition of the developable surface is ensured by incorporating the constraints on the principal curvature. The effectiveness of the present approach is confirmed through several numerical examples, and the characteristics of the results are discussed.

1. INTRODUCTION

Advancement of computer technologies as well as the developments of structural materials and construction methods enabled us to design so called *free-form shell*, which has complex shape and topology that cannot be categorized to traditional shapes. However, the mechanical behavior of such shell is very complicated, and it is very difficult for a designer to decide feasible shape of a real-world structure based on his/her experience and intuition as a compromise of aesthetical property and mechanical rationality. Furthermore, it is very important in practical design that the smoothness of the shape should be maintained while moderately complex geomerty is searched. In this respect, qualitative measures for defining roundness may be effectively utilized[1, 2]. However, there are other measures of smoothness to be considered by the designers.

In this study, a new approach is proposed for shape optimization of shells modeled using Bézier surface. The strain energy is used to represent the mechanical performance, and the aesthetic aspects and smoothness of the surface are quantified by algebraic invariants of the surface representing curvature, convexity, gradient, etc. The condition of the developable surface is ensured by incorporating the constraints on the principal curvature.

2. SHAPE REPRESENTATION BY BÉZIER SURFACE

The number of variables for optimization can be drastically reduced without sacrificing smoothness and complexity of the surface using the Bézier surface. Moreover, the basis functions of Bézier surface can be expressed explicity with respect to the coordinates of the control points, which enables us to carry out sensitivity analysis of the algebraic invariants analytically. The point $\boldsymbol{S}_{I,J}(s,t) = [x(s,t), y(s,t), z(s,t)]^\top$ on a tensor product Bézier surface is defined with parameters $s, t \in [0,1]$ as

$$\boldsymbol{S}_{I,J}(s,t) = \sum_{i=0}^{I}\sum_{j=0}^{J} \boldsymbol{q}_{ij} B_{I,i}(s) B_{J,j}(t) \tag{1}$$

where $\boldsymbol{q}_{ij} = [q_{x,ij}, q_{y,ij}, q_{z,ij}]^\top$ is the control point, and $B_{I,i}(s)$ and $B_{J,j}(t)$ are the Bernstein basis functions. I and J are the orders of the functions. The vector of x-coordinates of control points is defined as

$$\boldsymbol{q}_x = [q_{x,00}, \cdots, q_{x,0J}, \cdots, q_{x,I0}, \cdots, q_{x,IJ}]^\top \tag{2}$$

$\boldsymbol{q}_y$ and $\boldsymbol{q}_z$ are defined similarly.

In order to evaluate the static responses of the shells using finite element method, we divide the surface of (1) into $I' \times J'$ grid with uniformly spaced parameters t and s, respectively, and the vector $\boldsymbol{r}_x$ of the x-coordinates of the nodes is defined as

$$\boldsymbol{r}_x = [x(s_0, t_0), \cdots, x(s_0, t_{I'}), \cdots, x(s_{I'}, t_0), \cdots, x(s_{I'}, t_{J'})]^\top \tag{3}$$

$\boldsymbol{r}_y$ and $\boldsymbol{r}_z$ are defined similarly. The coordinate vector of a node on the surface can be written as follows:

$$\boldsymbol{S}_{I,J}(s_k, t_l) = \sum_{i=0}^{I}\sum_{j=0}^{J} \boldsymbol{q}_{ij} B_{I,i}(s_k) B_{J,j}(t_l), \quad (k = 0, \cdots, I';\ l = 0, \cdots, J') \tag{4}$$

3. β INVARIANTS AND γ INVARIANTS

We use the six algebraic invariants β_0, β_1, β_2, γ_1, γ_2, and γ_3 proposed by Iri *et al.* [3] for representing the geographical propeties. Here, we regard $z(s,t)$ of the Bézier surface (1) as the altitude of the geographical representation.

3.1 Definitions of tensors and vectors

In the following, the covariant and the contravariant components are indicated by the subscript and superscript, respectively. The components of the covariant gradient vector $\underline{\boldsymbol{z}}$, the covariant hessian $\underline{\boldsymbol{h}}$, and the covariant metric tensor $\underline{\boldsymbol{g}}$ are defiend

$$\underline{\boldsymbol{z}} = \begin{bmatrix} z_s \\ z_t \end{bmatrix}, \quad \underline{\boldsymbol{h}} = \begin{bmatrix} h_{ss} & h_{st} \\ h_{ts} & h_{tt} \end{bmatrix}, \quad \underline{\boldsymbol{g}} = \begin{bmatrix} g_{ss} & g_{st} \\ g_{ts} & g_{tt} \end{bmatrix} \tag{5}$$

which are obtained from

$$z_s = \frac{\partial z(s,t)}{\partial s} = \sum_{i=0}^{I}\sum_{j=0}^{J} q_{z,ij}\frac{\partial B_{I,i}(s)}{\partial s}B_{J,j}(t), \quad z_t = \frac{\partial z(s,t)}{\partial t} = \sum_{i=0}^{I}\sum_{j=0}^{J} q_{z,ij}B_{I,i}(s)\frac{\partial B_{J,j}(t)}{\partial t} \tag{6}$$

$$\begin{aligned} h_{ss} &= \frac{\partial^2 z(s,t)}{\partial s^2} = \sum_{i=0}^{I}\sum_{j=0}^{J} q_{z,ij}\frac{\partial^2 B_{I,i}(s)}{\partial s^2}B_{J,j}(t), \quad h_{tt} = \frac{\partial^2 z(s,t)}{\partial t^2} = \sum_{i=0}^{I}\sum_{j=0}^{J} q_{z,ij}B_{I,i}(s)\frac{\partial^2 B_{J,j}(t)}{\partial t^2} \\ h_{st} = h_{ts} &= \frac{\partial^2 z(s,t)}{\partial s \partial t} = \sum_{i=1}^{I}\sum_{j=1}^{J} q_{z,ij}\frac{\partial B_{I,i}(s)}{\partial s}\frac{\partial B_{J,j}(t)}{\partial t} \end{aligned} \tag{7}$$

$$\begin{aligned} g_{ss} &= \frac{\partial \boldsymbol{S}_{I,J}(s,t)}{\partial s}^{\top}\frac{\partial \boldsymbol{S}_{I,J}(s,t)}{\partial s}, \qquad g_{tt} = \frac{\partial \boldsymbol{S}_{I,J}(s,t)}{\partial t}^{\top}\frac{\partial \boldsymbol{S}_{I,J}(s,t)}{\partial t} \\ g_{st} = g_{ts} &= \frac{\partial \boldsymbol{S}_{I,J}(s,t)}{\partial s}^{\top}\frac{\partial \boldsymbol{S}_{I,J}(s,t)}{\partial t} \end{aligned} \tag{8}$$

Let $\overline{\boldsymbol{z}}$ and $\overline{\boldsymbol{g}}$ denote the contravariant gradient vector of z-coordinate and the contravariant metric tensor, respectively. Then the following relations holds:

$$\overline{\boldsymbol{g}} = \underline{\boldsymbol{g}}^{-1}, \ \overline{\boldsymbol{z}} = \overline{\boldsymbol{g}}\underline{\boldsymbol{z}}, \quad \underline{\boldsymbol{z}} = \underline{\boldsymbol{g}}\overline{\boldsymbol{z}} \tag{9}$$

In addition, we define the following contravariant vector $\tilde{\boldsymbol{z}}$:

$$\tilde{\boldsymbol{z}} = \begin{bmatrix} \tilde{z}^s \\ \tilde{z}^t \end{bmatrix} = \tilde{\boldsymbol{E}}\underline{\boldsymbol{z}}, \quad \tilde{\boldsymbol{E}} = \begin{bmatrix} \tilde{E}^{11} & \tilde{E}^{12} \\ \tilde{E}^{21} & \tilde{E}^{22} \end{bmatrix} = \begin{bmatrix} 0 & 1 \\ -1 & 0 \end{bmatrix} \tag{10}$$

The product of a covariant vector and a contravariant vector, and the bilinear form with respect to a second-order covariant/contravariant tensor and a conrtavariant/cobariant vector are invariant with respect to the definition of the parameter of the surface. Then, β and γ invariants are defined as follows:

$$\beta_0 = \sum_{\xi=s,t}\sum_{\lambda=s,t} g^{\xi\lambda}z_\xi z_\lambda = \sum_{\xi=s,t} z^\xi z_\xi \ (\geq 0) \tag{11}$$

$$\beta_1 = \sum_{\xi=s,t}\sum_{\lambda=s,t} h_{\lambda\xi}g^{\xi\lambda} \tag{12}$$

$$\beta_2 = \frac{1}{2\det(\underline{\boldsymbol{g}})}\sum_{\xi=s,t}\sum_{\lambda=s,t}\sum_{\mu=s,t}\sum_{\nu=s,t} h_{\nu\lambda}h_{\mu\xi}\tilde{E}^{\xi\lambda}\tilde{E}^{\mu\nu} \tag{13}$$

$$\gamma_1 = \sum_{\lambda=s,t}\sum_{\xi=s,t} h_{\lambda\xi}z^\xi z^\lambda \tag{14}$$

$$\gamma_2 = \sum_{\lambda=s,t}\sum_{\xi=s,t} h_{\lambda\xi}\tilde{z}^\xi z^\lambda = \sum_{\lambda=s,t}\sum_{\xi=s,t} h_{\lambda\xi}z^\xi \tilde{z}^\lambda \tag{15}$$

$$\gamma_3 = \frac{1}{\det(\underline{\boldsymbol{g}})}\sum_{\lambda=s,t}\sum_{\xi=s,t} h_{\lambda\xi}\tilde{z}^\xi \tilde{z}^\lambda \tag{16}$$

3.2 SURFACE PROPERIES BASED ON ALGEBRAIC INVARIANTS

The six algebraic invariants $\beta_0, \beta_1, \beta_2, \gamma_1, \gamma_2$, and γ_3, defined using the vectors and tensors given in Sec.3.1, are used for quantitative evaluation of the surface properties. The local properties in the neighborhood of a point P on the surface are characterized by the invariants as follows:

$\underline{\beta_2 > 0}$ The contours in the neighbourhood of P are coaxial (part of) similar ellipses. Especially, when $\beta_1^2 = 4\beta_2$, the contours are (part of) concentric circles and the surface is locally isotropically curved. The shape is locally concave if $\beta_1 > 0$, and locally convex if $\beta_1 < 0$.

$\underline{\beta_2 < 0}$ The contours in the neighbourhood of P are (part of) coaxial hyperbolas. Locally, the surface is convex in some directions and concave in others. There are special directions in which the contour lines are straight (i.e., neither concave nor convex).

$\underline{\beta_2 = 0}$ One of the principal curvatures is 0. Furthermore, the other principal curvature is positive if $\beta_1 > 0$; and negative if $\beta_1 < 0$; and 0 if $\beta_1 = 0$ that means a locally flat surface.

$\underline{\beta_0 = 0}$ P is a critical point (locally maximum/minimum value of z-coordinate).

$\underline{\gamma_2 = 0}$ Direction of gradient vector coincides with one of the principal direction, and the surface near P is locally cylindrical and concave in one principal direction if $|\gamma_1| < |\gamma_3|$ and $|\gamma_3 = 0|$; wheras it is locally cylindrical and convex in one principal direction if $|\gamma_1| > |\gamma_3|$ and $|\gamma_3 = 0|$.

In addition, β_1 and β_2 correspond to the twice the average curvature and the Gaussian curvature, respectively. Furthermore, γ_1/β_0 is the curvature in the steepect desent direction, and γ_3/β_0 is the curvature in its perpendicular direction.
In view of constructability, it is desirable that the surface can be developed to a plane without expansion or contraction. Such surface is called developable surface, which is characterized by vanishing Gaussian curvature. Therefore, to generate a developable surface, the constraint $\beta_2 = 0$ should be satisfied at any point on the surface.

4. NUMERICAL EXAMPLES

4.1 Sescription of shell model and optimization problem

The shape of the shell structure that has the square plane as shown in Fig.1(a) is optimized considering the algebraic invariants and the strain energy under self-weight. Each of four corners have a pair of pin supports to avoid the stress concentration.
The initial values of the control points are defined so as to closely represent the bi-directional quadratic function $z = h(x^2 - a^2)(y^2 - b^2)$, where the origin of the coordinate system is the center of the square including the supports. The span is 30 m and rize is 6 m; i.e., $a = b = 15$, $h = 6/a^2b^2$. Based on the symmetry condition, the optimal shapes are found for Bézier patch representing the 1/4 part of the shell as shown in Fig.1(b).

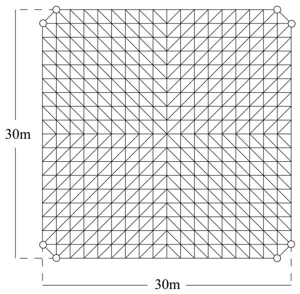

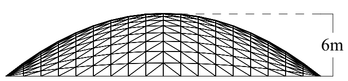

Rize	[m]	6.00
Young's modulus	[GPa]	21.00
Poison ratio		0.17
Unit weight	[kN/m3]	24.00
Tickness(uniformity)	[m]	0.10
Area	[m2]	989.77

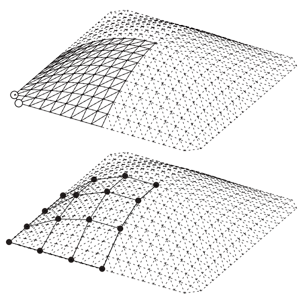

(a) Plan, view, and various amounts of shape (b) 1/4 area bézier patch

Fig.1. Analytical model

The uniform thickness of the shell is 0.1 m, weight density is 24k N/m^3. Young's modulus and Poisson's ratio are 21 GPa and 0.17, respectively. Displacements and stresses under self-weight are calculated by linear static finite element analysis. The constant strain triangular element[4)] is adopted for the in-plane deformation and nonconforming triangle element proposed by Zienkiewics *et al.* [5)] is adopted for the out-of-plane deformation.

The design variables are the z-coordinates $\boldsymbol{q}_z$ of the control points of the Bézier surface for the 1/4 part; hence, the number of variables 16. Because Bézier patch shuts in 1/4 areas, the continuousness of the gradient and the curvature in the boundary part is not necessarily kept. The number of nodes for the analysis is 99 because it does in 1/4 areas about the structure analysis in consideration of symmetry.

The optimum shape is found under constraints on the coordinates of the supports and the algebraic invariants. Moreover, to prevent unrealistic shape with extremely large rise, and to improve the convergence property of optimization algorithm, an upper bound is given for the area of shell's middle surface (henceforth area). Since the shell has a uniform thickness, the area constraint is equivalent to the volume or weight constraint that is usually regarded as representing the material cost.

In each of the optimization problem formulated below, total number of degrees of freedom, nodal displacement vector, linear stiffness matrix, area, and vector consisting of z-coordinates of the supports are denoted by n, $\boldsymbol{d} \in R^n$, $\boldsymbol{K} \in R^{n\times n}$, S, and $\boldsymbol{r}_z^* \in R^2$, respectively. The value of the initial shape is shown by 0 subscript. The sequential quadratic programming method in SNOPT[6)] is used for optimization.

4.2 Optimal shape without constraints on algebraic invariants

We first find optimal shape without constraints on algebraic invariants. The strain energy is minimized as follows under constraints on the locations of the supports, and the upper-bound constraint on the area:

$$\begin{aligned} &\text{minimize} \quad f(\boldsymbol{q}_z) = \frac{1}{2}\boldsymbol{d}^\top \boldsymbol{K}\boldsymbol{d} \\ &\text{subject to} \quad \begin{cases} S - S_0 \leq 0 \\ \boldsymbol{r}_z^* - \boldsymbol{r}_{z,0}^* = 0 \end{cases} \end{aligned} \tag{17}$$

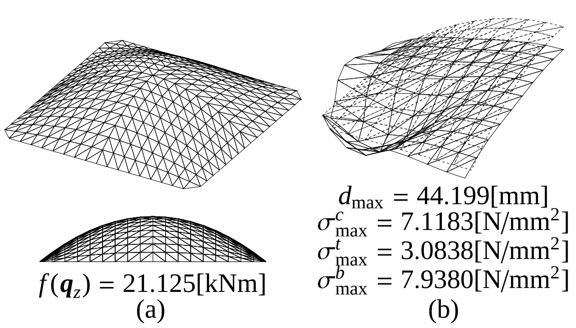

Fig.2. Initial shape

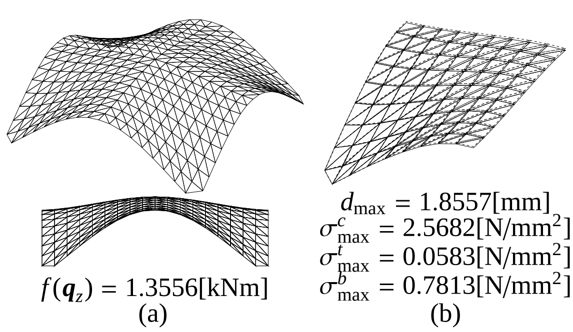

Fig.3. Optimal shape

The initial and optimal shapes are shown in Figs.2(a) and 3(a), respectively. The dashed and solid lines, respectively, in Figs.2(b) and 3(b) are the undeformed and deformed shapes, where the displacements are magnified by the factor 100. The optimal objective value $f(\boldsymbol{q}_z)$, maximum values of displacement $d_{\max}$, compressive stress $\sigma^c_{\max}$, tensile stress $\sigma^t_{\max}$, and bending stress $\sigma^b_{\max}$ are also shown in the figures. It can be confirmed from the optimization result that bending and tensile stresses are reduced and the shape is optimized so that the shell resists the self-weight mainly with compression.

4.3 Optimal shape without constraints on $\boldsymbol{\beta}$ invariants

We next consider the following optimization problem by introducing the constraints on $\boldsymbol{\beta}$ invariants to obtain a locally convex surface:

$$
\begin{aligned}
&\text{minimize} \quad f(\boldsymbol{q}_z) = \frac{1}{2}\boldsymbol{d}^\top \boldsymbol{K}\boldsymbol{d} \\
&\text{subject to} \quad \begin{cases} S - S_0 \leq 0 \\ \boldsymbol{r}^*_z - \boldsymbol{r}^*_{z,0} = 0 \\ \beta^c_2 > 0 \\ \beta^c_1 \leq \overline{\beta} \end{cases}
\end{aligned}
\tag{18}
$$

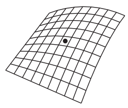

β^c_2 : $\beta_2$value at point c
β^c_1 : $\beta_1$value at point c
c : Invariants constraints point
$(s^c, t^c) = (0.5, 0.5)$

where $\overline{\beta} < 0$ to ensure convexity around point c indicated by the dot in the figure.

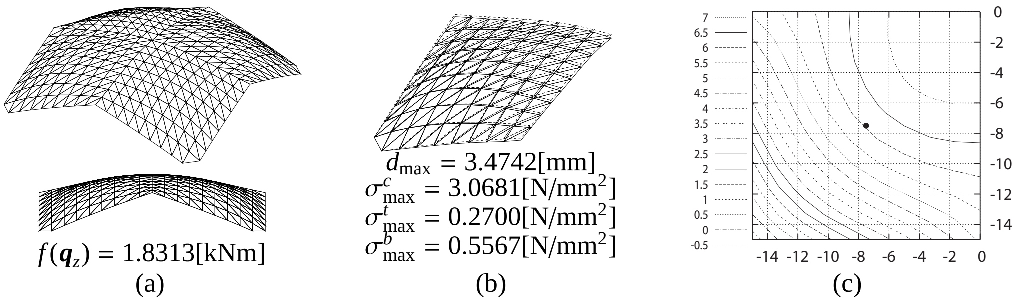

Fig.4. Optimal shape ($\overline{\beta} = -0.1$)

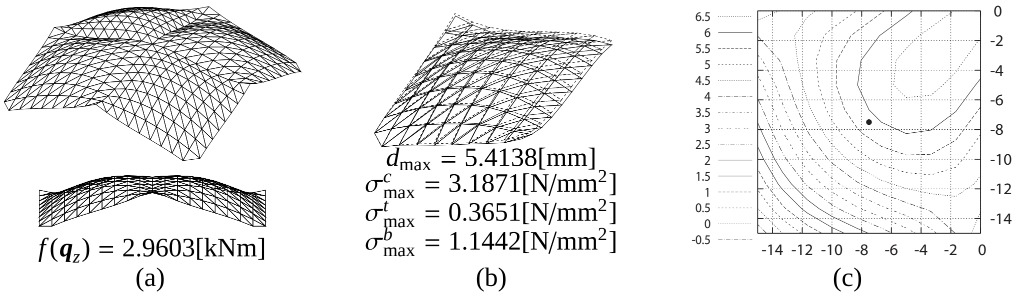

Fig.5. Optimal shape ($\overline{\beta} = -0.15$)

Figs.4 and 5 show the optimization results for $\overline{\beta} = -0.1$ and -0.15, respectively. Contour lines of the z-coordinates are plotted in Figs.4(c) and 5(c). As is seen, the masimum values of displacement, compressive stress, and tensile stress increase as a result of assigning requirement of local convexity. The displacement and stresses also increase by increasing the absolute value of β^c_1.

4.4 Optimal shape without constraints on γ invariants

We next solve the following problem with constraints on $\boldsymbol{\gamma}$ invariants to obtain locally cylindrical and convex surface:

$$
\begin{aligned}
&\text{minimize} \;\; f(\boldsymbol{q}_z) = \frac{1}{2}\boldsymbol{d}^{\top}\boldsymbol{K}\boldsymbol{d} \\
&\text{subject to} \;\; \begin{cases} S - S_0 \leq 0 \\ \boldsymbol{r}_z^* - \boldsymbol{r}_{z,0}^* = 0 \\ \gamma_2^{ci} = 0 \\ \gamma_3^{ci\,2} - \gamma_1^{ci\,2} > 0 \\ \gamma_3^{ci} \leq \overline{\gamma}^{ci} \\ {\scriptstyle (i=1,2)} \end{cases}
\end{aligned}
\tag{19}
$$

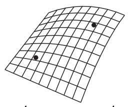

γ_2^{ci} : $\gamma_2$value at point ci

γ_1^{ci} : $\gamma_1$value at point ci

ci : Invariants constraints point

$(s^{c1}, t^{c1}) = (0.25, 0.25)$

$(s^{c2}, t^{c2}) = (0.75, 0.75)$

where the constraints on the γ invariants are given at points $c1$ and $c2$ indicated by dots in the figure.

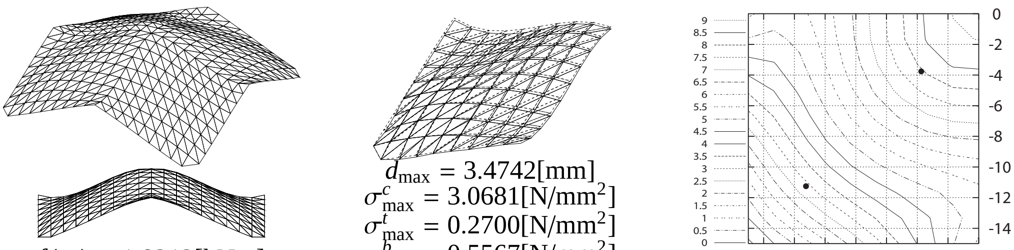

$f(\boldsymbol{q}_z) = 1.8313$[kNm]

(a)

$d_{\max} = 3.4742$[mm]
$\sigma^c_{\max} = 3.0681$[N/mm^2]
$\sigma^t_{\max} = 0.2700$[N/mm^2]
$\sigma^b_{\max} = 0.5567$[N/mm^2]

(b)

(c)

Fig.6. Optimal shape ($\overline{\gamma}^{c1} = \overline{\gamma}^{c2} = -0.015$)

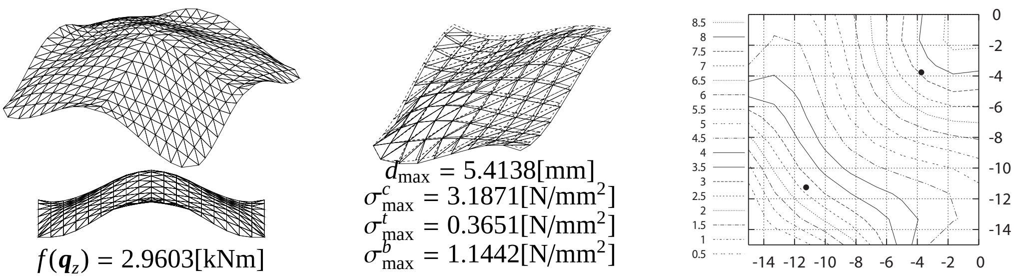

$f(\boldsymbol{q}_z) = 2.9603$[kNm]

(a)

$d_{\max} = 5.4138$[mm]
$\sigma^c_{\max} = 3.1871$[N/mm^2]
$\sigma^t_{\max} = 0.3651$[N/mm^2]
$\sigma^b_{\max} = 1.1442$[N/mm^2]

(b)

(c)

Fig.7. Optimal shape ($\overline{\gamma}^{c1} = \overline{\gamma}^{c2} = -0.025$)

Figs.6 and 7 show the optimization results for $\overline{\gamma}^{c1} = \overline{\gamma}^{c2} = -0.015$ and $\overline{\gamma}^{c1} = \overline{\gamma}^{c2} = -0.025$, respectively. It can be confirmed that a locally cylindrical and convex surface has been successfully obtained by introducing the constraints on the γ invariants.

4.5 Optimal shape with developability constraints

Finally, we generate a developable surface by shape optimization. The following problem is to be solved so that β_2 vanishes at 25 points indicated by the dots in the figure:

$$
\begin{aligned}
&\text{minimize} \;\; f(\boldsymbol{q}) = \frac{1}{2}\boldsymbol{d}^{\top}\boldsymbol{K}\boldsymbol{d} \\
&\text{subject to} \;\; \begin{cases} S - S_0 \leq 0 \\ \beta_2^{ci} = 0 \\ {\scriptstyle (i=1,\cdots,25)} \end{cases}
\end{aligned}
\tag{20}
$$

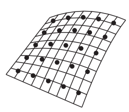

β_2^{ci} : $\beta_2$value at point ci

ci : Invariants constraints point

$s^{ci}, t^{ci} \in [0.1, 0.3, 0.5, 0.7, 0.9]$

The optimal shape is shown in Fig.8. It can be seen from Fig.8(c) that maximum value of β_2^{ci} has been successfully minimized, although there is no guarantee that β_2 becomes 0 at the points

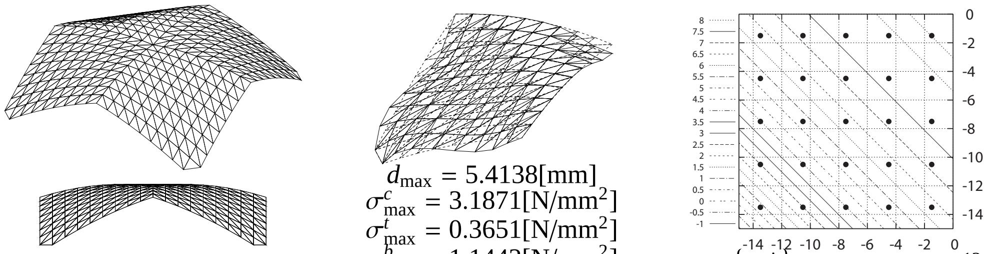

$f(\boldsymbol{q}_z) = 2.9603$[kNm]
(a)

$d_{\max} = 5.4138$[mm]
$\sigma^c_{\max} = 3.1871$[N/mm^2]
$\sigma^t_{\max} = 0.3651$[N/mm^2]
$\sigma^b_{\max} = 1.1442$[N/mm^2]
(b)

$\max\left\{|\beta_2^{ci}|\right\} = 5.3285 \times 10^{-12}$
(c)

Fig.8. Optimal shape

where the constraints are not given. The contour lines became almost straight and parallel It can be confirmed from Fig.8(a) that each of the 1/4 part seem to be deveopable. Furthermore, both of the strain energy and the maximum vertical displacement have smaller values than the initial shape.

5. CONCLUSIONS

The local properties of the shell surface can be explicitly controled by solving an optimization problem with constraints on the algebraic invariants of the surface. Moreover, a developable surface can be obtained by assigning the constraint such that the Gaussian curvature vamishes everywhere on the surface.

It may be concluded that the algebraic invariants are effective indices representing the local properties of the surface, and the optimal shell shape considering the aesthetic aspects, constructability and mechanical rationality can be generated using the proposed approach at the early design stage.

REFERENCES

1. M. Ohsaki and M. Hayashi, Fairness metrics for shape optimization of ribbed shells, *J. Int. Assoc. Shells and Spatial Struct.*, 2000, Vol. 41(1), pp. 31–39
2. M. Ohsaki, T. Ogawa and R. Tateishi, Shape optimization of curves and surfaces considering fairness metrics and elastic stiffness, *Struct. Multidisc. Optim.*, 2003, Vol. 24, pp. 449–456, Erratum: 2004, Vol. 27, pp. 250–258
3. M. Iri, Y. Shimakawa, and T. Nagai, Extraction of invariants from digital elevation data with application to terrain topography, *Nonlinear Analysis*, 2001, Vol.47, pp. 5585–5598
4. S. Timoshenko, and K. Woinowsky, *Theory of plates and shells*, McGraw-Hill, 1959
5. G. P. Bazeley, Y. K. Cheung, B. M. Irons, and O. C. Zienkiewicz, Triangular elements in bending–conforming and nonconforming solutions, *Proceedings of the Conference on Matrix Methods in Structural Mechanics*, 1959, pp.547–576
6. P. Gill, W. Murray, and M. Saunders, *User's Guide for snopt Version 7 : Software for Large-Scale Nonlinear Programming*, Stanford Business Software Inc., 2008